

Breaking the Orthogonality Barrier in Quantum LDPC Codes

Kenta Kasai
 Institute of Science Tokyo
 kenta@ict.eng.isct.ac.jp

Abstract

Classical low-density parity-check (LDPC) codes are a widely deployed and well-established technology, forming the backbone of modern communication and storage systems. It is well known that, in this classical setting, increasing the girth of the Tanner graph while maintaining regular degree distributions leads simultaneously to good belief-propagation (BP) decoding performance and large minimum distance. In the quantum setting, however, this principle does not directly apply because quantum LDPC codes must satisfy additional orthogonality constraints between their parity-check matrices. When one enforces both orthogonality and regularity in a straightforward manner, the girth is typically reduced and the minimum distance becomes structurally upper bounded.

In this work, we overcome this limitation by using permutation matrices with controlled commutativity and by restricting the orthogonality constraints to only the necessary parts of the construction, while preserving regular check-matrix structures. This design breaks the conventional trade-off between orthogonality, regularity, girth, and minimum distance, allowing us to construct quantum LDPC codes with large girth and without the usual distance upper bounds. As a concrete demonstration, we construct a girth-8, (3,12)-regular $[[9216, 4612, \leq 48]]$ quantum LDPC code and show that, under BP decoding combined with a low-complexity post-processing algorithm, it achieves a frame error rate as low as 10^{-8} on the depolarizing channel with error probability 4%.

1 Introduction

Classical low-density parity-check (LDPC) codes are a widely deployed and well-established technology in modern communication and storage systems [1], and BP decoding can achieve channel capacity [2, 3]. Performance depends strongly on the Tanner-graph degree distribution: regular codes can perform well, and carefully designed irregular distributions can further improve BP performance [4], whereas naive regularization can degrade it. Random LDPC codes with variable-node degree at least 3 have minimum distance growing linearly with blocklength [5, 1], so classical LDPC research has not focused on increasing minimum distance itself. Moreover, BP decoding can be trapped by small Tanner-graph structures called trapping sets [6], which cause decoding failures; suppressing harmful trapping sets typically requires large girth [7].

Sparse-graph quantum error-correcting codes were proposed in [8], and the behavior of iterative decoding and the role of degeneracy were discussed in [9]. Families with positive rate and distance $\Theta(\sqrt{n})$ are known [10]. Constructions based on Kronecker sum and product [11], distance bounds for generalized bicycle (GB) codes [12], finite-length evaluations [13], and decoding protocols [14] have been reported, advancing the theoretical understanding of CSS-type QLDPC codes. However, the orthogonality constraint between the CSS parity-check matrices H_X and H_Z , namely $H_X H_Z^\top = 0$, has no classical counterpart, and enforcing both orthogonality and regularity in a straightforward manner typically reduces girth and induces structural distance upper bounds.

Surface codes and hypergraph product (HGP) codes rely on geometric or product structures and thus follow design principles different from those developed for classical LDPC codes. As a result, it is not straightforward to apply classical degree-distribution and girth design techniques directly [15, 10, 5]. The goal of this work is to provide a construction principle that preserves classical LDPC parity-check structures while enabling their direct use as CSS check matrices. Specifically, we aim for regular LDPC codes with large girth and variable degree at least 3, whose minimum distance is not trivially upper bounded.

Prior work has explored cyclic parity-check matrices that allow explicit control of regular Tanner-graph degree distributions. Representative constructions include the Hagiwara–Imai codes [16] and bicycle constructions [8, 11, 12]. However, these constructions have known limitations. Even for classical codes, one-step lifting of a protograph (lifting by circulant permutation matrices (CPMs)) can impose fixed upper bounds on girth due to the protograph structure. Mitchell et al. pointed out that one-step lifting can impose fixed bounds on minimum distance and girth and that two-step lifting can improve them [17]. For CSS codes, the parity-check matrices H_X and H_Z are QC, and the Tanner-graph girth satisfies $g = \min\{g(H_X), g(H_Z)\}$, so QC girth bounds apply to each matrix. For quasi-cyclic CSS designs, generalized CSS (entanglement-assisted) constructions use classical QC constructions with girth ≥ 6 to avoid 4-cycles [18]. Explicit constructions achieving girth 12 for column weight 2 have also been reported [19]. Moreover, for general quantum CPM–LDPC codes, the girth is upper bounded by 12 for column weight 2 and by 6 for column weight at least 3 [20]. Using APM–LDPC codes, these upper bounds can be broken [19, 21].

In CSS-type LDPC constructions, deleting rows from the parity-check matrices H_X or H_Z preserves the commutation condition $H_X H_Z^\top = 0$, but it weakens stabilizer constraints and can enlarge the code space [8, 16]. Row deletion is used for rate adjustment and for controlling row and column weights, yet distance preservation is not guaranteed in general [16, 22]. In particular, deleting rows can allow low-weight vectors to enter $C_X \setminus C_Z^\perp$ or $C_Z \setminus C_X^\perp$, creating new low-weight logical operators and thus reducing the minimum distance. In CSS codes, with $C_X = \ker(H_X)$ and $C_Z = \ker(H_Z)$, low-weight vectors in $C_X \setminus C_Z^\perp$ or $C_Z \setminus C_X^\perp$ become non-trivial logical operators [23, 24, 25]. Consequently, deleted check rows (which are LDPC and thus low weight) can become logical operators and upper bound the distance by the row weight. In the CSS product-code constructions of Ostrev et al., row removal is explicitly used to control the number of stabilizers, and distance degradation can occur [22]. Lin et al. report that removing redundant stabilizer rows reduces the syndrome distance, which is a structural effect due to fewer constraints, not a decoder artifact [14].

In this work, we first discuss the general mechanism by which row deletion can degrade the minimum distance of CSS codes. Next, for generalized Hagiwara–Imai codes [19], we establish a code-design method that controls commutativity of submatrices to avoid distance degradation due to row deletion. More concretely, using the algebraic structure of APM–LDPC codes, we guarantee orthogonality only on the active part, introduce a set of row pairs for which commutation is required, and localize the commutation condition. We further control the nonzero pattern of the interaction matrix so that deleted rows do not materialize as low-weight logical operators, and present a sequential construction algorithm based on the APM composition rule. As a concrete demonstration, we construct a (3,12)-regular [[9216, 4612, ≤ 48]] quantum LDPC code and show that, under BP decoding combined with a low-complexity post-processing algorithm, it achieves a frame error rate (FER) as low as 10^{-8} on the depolarizing channel with error probability 4%. We also compare constructions with and without commutation control to demonstrate suppression of low-weight logical operators.

2 Problem setting: low-weight logical operators induced by check-row removal

We abstract the conventional CSS–LDPC construction used in this paper, based on [8, 16]. We first construct two orthogonal square (block-circulant) mother matrices \hat{H}_X, \hat{H}_Z . The CSS code defined by these mother matrices typically has rate zero, so to adjust the rate we delete internal rows and use the remaining rows as the active matrices H_X and H_Z . Namely,

$$\hat{H}_X = \begin{bmatrix} H_X \\ \tilde{H}_X \end{bmatrix}, \quad \hat{H}_Z = \begin{bmatrix} H_Z \\ \tilde{H}_Z \end{bmatrix}$$

We refer to H_X and H_Z as the active part and \tilde{H}_X and \tilde{H}_Z as the latent part.

However, in this construction, mother orthogonality imposes strong constraints on the latent rows and can degrade the minimum distance. The minimum distance is defined as $d_{\min} = \min\{d_X, d_Z\}$ with

$$d_Z := \min\{\text{wt}(\mathbf{z}) : \mathbf{z} \in C_X \setminus C_X^\perp\}, \quad d_X := \min\{\text{wt}(\mathbf{x}) : \mathbf{x} \in C_Z \setminus C_X^\perp\}.$$

Mother orthogonality

$$\hat{H}_X(\hat{H}_Z)^\top = 0$$

forces not only the active orthogonality between the active matrices H_X and H_Z , namely $H_X H_Z^\top = 0$, but also

$$H_X(\tilde{H}_Z)^\top = 0, \quad H_Z(\tilde{H}_X)^\top = 0$$

which implies $\text{Row}(\tilde{H}_X) \subset C_Z$ and $\text{Row}(\tilde{H}_Z) \subset C_X$. Thus each row \mathbf{x} of \tilde{H}_X satisfies $\mathbf{x} \in C_Z$, and each row \mathbf{z} of \tilde{H}_Z satisfies $\mathbf{z} \in C_X$. In general \mathbf{x} need not belong to C_X^\perp and \mathbf{z} need not belong to C_Z^\perp , in which case they become logical operators. The minimum row weight (in our construction, L) becomes an upper bound on d_X and d_Z .

In this work we also obtain the active matrices H_X, H_Z by deleting rows from the mother matrices, but we design them so that low-weight rows in the latent matrices are not orthogonal to H_Z or H_X , respectively. That is, for low-weight $\mathbf{x} \in \text{Row}(\tilde{H}_X)$ we enforce $H_Z \mathbf{x}^\top \neq 0$, and for low-weight $\mathbf{z} \in \text{Row}(\tilde{H}_Z)$ we enforce $H_X \mathbf{z}^\top \neq 0$, so that in particular $\text{Row}(\tilde{H}_X) \not\subset C_Z$ and $\text{Row}(\tilde{H}_Z) \not\subset C_X$. The same argument applies not only to individual latent rows but also to low-weight linear combinations.

Accordingly, we define latent-based upper bounds for the X and Z distances as

$$\begin{aligned} d_X^{(\text{lat})} &:= \min\{\text{wt}(\mathbf{x}) : \mathbf{x} \in \text{Row}(\tilde{H}_X) \cap C_Z \setminus C_X^\perp\}, \\ &= \min\{\text{wt}(\mathbf{x}) : \mathbf{x} \in C_Z, \mathbf{x} = (\tilde{H}_X)^\top \mathbf{u}, \text{ for some } \mathbf{u}, \mathbf{x} \notin C_X^\perp\}, \\ d_Z^{(\text{lat})} &:= \min\{\text{wt}(\mathbf{z}) : \mathbf{z} \in \text{Row}(\tilde{H}_Z) \cap C_X \setminus C_Z^\perp\}, \\ &= \min\{\text{wt}(\mathbf{z}) : \mathbf{z} \in C_X, \mathbf{z} = (\tilde{H}_Z)^\top \mathbf{v}, \text{ for some } \mathbf{v}, \mathbf{z} \notin C_Z^\perp\} \end{aligned}$$

The proposed design aims to make these bounds as large as possible. In [26], binary submatrices corresponding to codewords are lifted to a nonbinary field so that they no longer represent codewords; this can be viewed as increasing these latent-based bounds via nonbinary lifting.

3 Method of matrix design

In this section, based on the above problem setting, we aim to construct the latent matrices \tilde{H}_X and \tilde{H}_Z such that

$$H_X H_Z^\top = 0, \quad H_X (\tilde{H}_Z)^\top \neq 0, \quad H_Z (\tilde{H}_X)^\top \neq 0$$

and $d_X^{(\text{lat})}, d_Z^{(\text{lat})}$ are large. We define generalized Hagiwara–Imai codes, i.e., mother matrix pairs with block-circulant structure, and develop a general theory for imposing only the active orthogonality $H_X H_Z^\top = 0$ between the active matrices H_X and H_Z .

A protograph LDPC code with column weight J and row weight L is defined by a parity-check matrix consisting of $J \times L$ permutation matrices of size P [27]. For a permutation $f : [P] \rightarrow [P]$, the corresponding $P \times P$ permutation matrix $F = P(f)$ is defined by $F_{x,y} = 1 \iff f(x) = y$. Each row and column has exactly one 1, so the mother matrix is sparse while its block structure is compact.

We introduce generalized Hagiwara–Imai codes [19] as protograph generalizations of the Hagiwara–Imai quasi-cyclic CSS codes [16]. For permutation matrices F_i, G_i ($i \in [L_2]$) of size P , define the mother matrices \hat{H}_X, \hat{H}_Z of size $(L_2 P) \times (LP)$ by

$$\begin{aligned} (\hat{H}_X)_{i,j} &= F_{j-i}, & (\hat{H}_X)_{i,L_2+j} &= G_{j-i}, \\ (\hat{H}_Z)_{i,j} &= (G_{i-j})^\top, & (\hat{H}_Z)_{i,L_2+j} &= (F_{i-j})^\top. \end{aligned}$$

All subscripts are taken modulo L_2 . Throughout, indices in $[L/2]$ are taken modulo $L/2$, i.e., we identify $[L/2]$ with $\mathbb{Z}_{L/2}$. A sufficient condition for orthogonality is given below. The active matrices H_X and H_Z consist of the top J block rows. Conventional designs impose commutativity of F_i and G_j so that both H_X, H_Z and \hat{H}_X, \hat{H}_Z are orthogonal. The top J block rows of the mother matrices are used as the active matrices H_X and H_Z . Our interest is to satisfy active orthogonality $H_X H_Z^\top = 0$ while not imposing mother-matrix orthogonality.

Each block row of \hat{H}_X is a cyclic shift of $(F_0, F_1, \dots, F_{L/2-1})$ in the left half and $(G_0, G_1, \dots, G_{L/2-1})$ in the right half. Hence blocks depend only on the difference $(j-i)$, and the product of mother matrices depends only on the difference. For any $i, k \in [L_2]$, the (i, k) block is

$$(\hat{H}_X (\hat{H}_Z)^\top)_{i,k} = \sum_{u=0}^{L_2-1} (F_u G_{k-u} + G_{k-u} F_u) =: \Psi_r$$

which depends only on $r = (k-i) \bmod L_2$. For $r \in [L/2]$, if F_u and G_{r-u} commute for all $u \in [L/2]$, then $\Psi_r = 0$.

3.1 Sufficient condition for active orthogonality

We re-derive a convenient form of a sufficient condition for $H_X H_Z^\top = 0$ [26]. Define

$$\Delta := \{(k-i) \bmod L/2 \mid 0 \leq i, k \leq J-1\} \subseteq [L/2].$$

The next theorem spells out how commutativity restricted to these differences guarantees active orthogonality.

Theorem 3.1. If F_u and G_{r-u} commute for all $r \in \Delta$ and all $u \in [L/2]$, then $H_X H_Z^\top = 0$.

Proof. For any $i, k \in [J]$, we have $r = (k-i) \bmod L/2 \in \Delta$. By assumption, $\Psi_r = 0$, hence for all $i, k \in [J]$, $(\hat{H}_X (\hat{H}_Z)^\top)_{i,k} = \Psi_{(k-i) \bmod L/2} = 0$. Therefore $H_X H_Z^\top = 0$. \square

3.2 Necessary condition for latent non-orthogonality

Define the index pairs of (F_i, G_j) required to commute by

$$\Gamma := \bigcup_{r \in \Delta} \Gamma_r, \quad \Gamma_r := \{(i, j) \mid (i, j) = (u, r - u), u \in [L/2]\}$$

where subscripts are modulo $L/2$. Here Γ_r is the set of index pairs contributing to Ψ_r , and $\Gamma_r \cap \Gamma_s = \emptyset$ for $r \neq s$.

If $J \geq L/2$ then the rate is zero, so we assume $J < L/2$. We first state a basic feasibility constraint: without enough blocks, latent non-orthogonality cannot be forced.

Theorem 3.2. Assume the active orthogonality $H_X H_Z^\top = 0$. For the standard active choice (top J block rows), to have $H_X(\tilde{H}_Z)^\top \neq 0$ and $H_Z(\tilde{H}_X)^\top \neq 0$, it is necessary that $L \geq 4J$.

Proof. Assume $L < 4J$. Then for this active choice, $\Delta = [L/2]$. Active orthogonality $H_X H_Z^\top = 0$ implies $\Psi_r = 0$ for all $r \in \Delta$, hence $\Psi_r = 0$ for all $r \in [L/2]$. Therefore every block of $\hat{H}_X(\hat{H}_Z)^\top$ vanishes, in particular the mixed blocks between active and latent rows, so $H_X(\tilde{H}_Z)^\top = 0$ and $H_Z(\tilde{H}_X)^\top = 0$, contradicting the premise. \square

We next isolate the minimal algebraic obstruction to latent non-orthogonality.

Theorem 3.3. To have $H_X(\tilde{H}_Z)^\top \neq 0$ and $H_Z(\tilde{H}_X)^\top \neq 0$, it is necessary that there exists $r \in [L/2] \setminus \Delta$ with $\Psi_r \neq 0$.

Proof. Assume $\Psi_r = 0$ for all $r \in [L/2] \setminus \Delta$. For any $i \in [L/2] \setminus [J]$ and $k \in [J]$, $r = (k - i) \bmod L/2$ does not belong to Δ . By assumption $\Psi_r = 0$, hence for all such i, k , $(\hat{H}_X(\hat{H}_Z)^\top)_{i,k} = \Psi_{(k-i) \bmod L/2} = 0$. Therefore $H_X(\tilde{H}_Z)^\top = 0$, and similarly $H_Z(\tilde{H}_X)^\top = 0$, a contradiction. If all pairs $(i, j) \in [L/2]^2 \setminus \Delta$ commute, then each term $F_u G_{r-u} + G_{r-u} F_u$ vanishes over \mathbb{F}_2 , so $\Psi_r = 0$ for all $r \notin \Delta$. \square

3.3 Upper bound on girth

Finally, we recall a structural limitation that applies when commutativity holds on all required differences.

Theorem 3.4. Let L be even and assume $2 \leq J \leq L/2$. If F_u and G_{r-u} commute for all $r \in \Delta$ and all $u \in [L/2]$, then the Tanner graphs of H_X and H_Z each contain an 8-cycle.

Proof. Since $J \geq 2$, we have $0, 1 \in \Delta$. Also $L/2 \geq 2$, so there exist $i \neq i'$ in $[L/2]$. Let $r = 0, s = 1$, and set $j = r - i, j' = s - i$ (indices modulo $L/2$). By definition, $(i, j), (i, j') \in \Gamma_r \cup \Gamma_s$, and similarly $(i', j), (i', j') \in \Gamma_r \cup \Gamma_s$. By assumption the corresponding F and G commute, so the 8-cycle word composed of the two F columns and two G columns is

$$W = F_i G_j^{-1} G_{j'} F_i^{-1} F_{i'} G_{j'}^{-1} G_j F_{i'}^{-1} \tag{1}$$

Using commutativity to reorder gives $W = (F_i F_i^{-1})(F_{i'} F_{i'}^{-1})(G_j^{-1} G_{j'}) (G_{j'}^{-1} G_j) = I$, so an 8-cycle necessarily exists in the Tanner graphs of H_X and H_Z . \square

4 Method of Matrix Construction

Building on the commutation conditions and active orthogonality derived in the previous section, we now present a concrete sequential procedure to construct permutation blocks that satisfy those constraints while avoiding short cycles. For a given $(L/2, P, J)$, we construct $\{F_i\}$ and $\{G_i\}$ that satisfy the following simultaneously:

- (1) F_i and G_j commute for $(i, j) \in \Delta$.
- (2) At least one $(i, j) \in [L/2]^2 \setminus \Delta$ is non-commuting.
- (3) Avoid short cycles in the active matrices H_X and H_Z .

The framework of constructing quasi-cyclic LDPC blocks from circulant permutation matrices (CPMs) was systematized by Fossorier [28]. We adopt affine permutation matrices (APMs): the APM-LDPC framework extends CPMs, and its algebraic form makes commutativity control straightforward via congruence conditions [29]. In the classical setting, Yoshida and Kasai reported that linear permutation polynomial (APM-based) codes achieve performance comparable to protograph LDPC codes [30], while no fixed girth upper bound has been reported for APM-based constructions, unlike one-step CPM lifting. Methods that combine APM-LDPC codes to extend length and girth have also been proposed [31]. From a group-theoretic viewpoint, APMs on \mathbb{Z}_P form the affine group $\text{AGL}(1, \mathbb{Z}_P) = \mathbb{Z}_P \rtimes \mathbb{Z}_P^\times$, a semidirect product of translations by the unit group; commutativity is therefore governed by the interaction between the linear and translation parts.

Consider an affine permutation (AP) on \mathbb{Z}_P ,

$$f(x) = ax + b, \quad a \in \mathbb{Z}_P^\times, \quad b \in \mathbb{Z}_P.$$

We set $f_i(x) = a_i x + b_i$ and $g_j(x) = c_j x + d_j$, and denote the corresponding permutation matrices by $F_i := P(f_i)$ and $G_j := P(g_j)$.

Under this representation, commutativity of APs can be checked by a quadratic congruence:

$$f_i g_j = g_j f_i \iff d_j(a_i - 1) - b_i(c_j - 1) \equiv 0 \pmod{P},$$

See [29] for a derivation. The condition involves products of a_i, c_j and b_i, d_j [29]. The commutation table can thus be expressed as a system of congruences; in particular, if a_i, c_j are chosen first, the commutation constraints reduce to linear congruences in b_i, d_j , enabling a consistent search [29, 31].

We sequentially select candidates that satisfy both the commutation table and short-cycle conditions, using backtracking when a candidate fails. The number of trials is adjusted dynamically based on recent success rates. We interpret each candidate generator as an arm in a multi-armed bandit and allocate trials accordingly [32].

Short-cycle detection reduces to checking fixed points of the composite map Σ along a block-cycle pattern [28, 29]. The AP composition is again AP, $\Sigma(x) = Ax + B$, so

$$\Sigma(x) = x \iff \gcd(A - 1, P) \mid B$$

provides a test without enumerating the Tanner graph [29].

5 Method of Decoding

Our experiments use BP decoding [8, 9] as the baseline. We first recall a basic principle: if we knew the support where the BP estimate differs from the true error, decoding would reduce to a linear

system on the corresponding columns, and a unique solution would imply successful recovery. For example, if the X -side mismatch support is E , then $H_Z(:, E) \mathbf{e}_E = \mathbf{r}_X$; if $H_Z(:, E)$ has full column rank, the solution is unique and yields the correct correction. The same applies to the Z side with H_X and \mathbf{r}_Z .

Let the BP estimate at each iteration be $\hat{\mathbf{x}}, \hat{\mathbf{z}}$. Define the residual syndromes

$$\mathbf{r}_X := \mathbf{s}_X \oplus H_Z \hat{\mathbf{x}}, \quad \mathbf{r}_Z := \mathbf{s}_Z \oplus H_X \hat{\mathbf{z}}.$$

Empirically, BP stalls or slowly oscillates roughly once per 10^5 trials, and we trigger post-processing in such cases. We invoke three post-processing methods: ETS-based post-processing, a correction based on flip history, and an OSD-based method. Below we briefly describe the procedure and the criteria. In post-processing, the residual syndrome \mathbf{r} is \mathbf{r}_X (with $H = H_Z$) or \mathbf{r}_Z (with $H = H_X$), depending on the side.

5.1 Flip history decoding

Flip history decoding (FHD) forms a candidate set F from variables that flipped during BP and seeks a correction that cancels the residual syndrome on the local submatrix. This local correction is a heuristic to resolve stalls caused by trapping structures [6]. Related local-flip decoders include weighted bit-flipping [33]. Concretely, let $N(F)$ be the set of check rows adjacent to F , and solve the GF(2) linear system

$$H_{N(F), F} \boldsymbol{\delta} = \mathbf{r}_{N(F)}.$$

If the system is solvable and the solution is unique, we flip the bits indicated by $\boldsymbol{\delta}$.

5.2 OSD

OSD [34] uses the least reliable variables from BP to form a column set K and solves

$$H_{:, K} \mathbf{x} = \mathbf{r}$$

using all rows. The method is applied independently to the X and Z sides. In the implementation, we perform a binary search on $|K|$ to find the minimum K that is solvable, then take the largest K within the range that preserves uniqueness. The correction is applied only when the solution weight is below a threshold.

5.3 Elementary Trapping Set (ETS)-based post-processing

ETS-based post-processing targets elementary trapping sets with $b = 2$ unsatisfied checks, which are among the most harmful structures that cause BP to stall. We precompute a library of ETSs from the Tanner graph (e.g., (6, 2), (8, 2), (10, 2)) and store each entry as a variable set V and its odd check pair (c_0, c_1) . During decoding, we run ETS-based post-processing only when the number of unsatisfied checks is small (we skip post-processing when the number is not small) and the residual syndrome has exactly two unsatisfied checks.

Given the current estimate, let \mathbf{r} be the residual syndrome and $U = \{c_0, c_1\}$ be its unsatisfied check pair. We scan ETS entries whose odd checks match U . For each candidate ETS with variable set V , we build the local check set $N(V)$ and reject it if \mathbf{r} has nonzero entries in $N(V) \setminus U$. Otherwise we solve the local system

$$H_{N(V), V} \boldsymbol{\delta} = \mathbf{r}_{N(V)}$$

over \mathbb{F}_2 using Gaussian elimination. If solvable, we flip variables in V according to $\boldsymbol{\delta}$ and accept the correction only when the syndrome matches the target. We try ETS sizes in increasing order and apply the first successful correction, independently for the X and Z sides.

6 Results

We instantiate the general theory of Section 3 and the sequential construction of Section 4 for the smallest case we were able to construct, $J = 3, L = 12, P = 768$. We first give explicit Δ, Γ and Ψ_r , clarify the active orthogonality condition for the active matrices H_X and H_Z , then design the commutation table and APM parameters, and finally evaluate distance bounds and FER.

6.1 Structure and active orthogonality

For $J = 3, L/2 = 6$, each block row is a cyclic shift of the previous row, so \hat{H}_X, \hat{H}_Z have a 6×12 block-circulant structure:

$$\hat{H}_X = \left(\begin{array}{cccccc|cccccc} F_0 & F_1 & F_2 & F_3 & F_4 & F_5 & G_0 & G_1 & G_2 & G_3 & G_4 & G_5 \\ F_5 & F_0 & F_1 & F_2 & F_3 & F_4 & G_5 & G_0 & G_1 & G_2 & G_3 & G_4 \\ F_4 & F_5 & F_0 & F_1 & F_2 & F_3 & G_4 & G_5 & G_0 & G_1 & G_2 & G_3 \\ \hline F_3 & F_4 & F_5 & F_0 & F_1 & F_2 & G_3 & G_4 & G_5 & G_0 & G_1 & G_2 \\ F_2 & F_3 & F_4 & F_5 & F_0 & F_1 & G_2 & G_3 & G_4 & G_5 & G_0 & G_1 \\ F_1 & F_2 & F_3 & F_4 & F_5 & F_0 & G_1 & G_2 & G_3 & G_4 & G_5 & G_0 \end{array} \right).$$

$$\hat{H}_Z = \left(\begin{array}{cccccc|cccccc} G'_0 & G'_5 & G'_4 & G'_3 & G'_2 & G'_1 & F'_0 & F'_5 & F'_4 & F'_3 & F'_2 & F'_1 \\ G'_1 & G'_0 & G'_5 & G'_4 & G'_3 & G'_2 & F'_1 & F'_0 & F'_5 & F'_4 & F'_3 & F'_2 \\ G'_2 & G'_1 & G'_0 & G'_5 & G'_4 & G'_3 & F'_2 & F'_1 & F'_0 & F'_5 & F'_4 & F'_3 \\ \hline G'_3 & G'_2 & G'_1 & G'_0 & G'_5 & G'_4 & F'_3 & F'_2 & F'_1 & F'_0 & F'_5 & F'_4 \\ G'_4 & G'_3 & G'_2 & G'_1 & G'_0 & G'_5 & F'_4 & F'_3 & F'_2 & F'_1 & F'_0 & F'_5 \\ G'_5 & G'_4 & G'_3 & G'_2 & G'_1 & G'_0 & F'_5 & F'_4 & F'_3 & F'_2 & F'_1 & F'_0 \end{array} \right).$$

Here, for simplicity, A' denotes the transpose of A . For example, the $(0, 1)$ block of $\hat{H}_X(\hat{H}_Z)^\top$ is

$$\begin{aligned} (\hat{H}_X(\hat{H}_Z)^\top)_{0,1} &= F_0G_1 + F_1G_0 + F_2G_5 + F_3G_4 + F_4G_3 + F_5G_2 \\ &\quad + G_0F_1 + G_1F_0 + G_2F_5 + G_3F_4 + G_4F_3 + G_5F_2 \\ &= \Psi_1. \end{aligned}$$

With $\Delta = \{0, 1, 2, 4, 5\}$,

$$\Gamma = \{(i, j) \in [L/2]^2 \mid i + j \not\equiv 3 \pmod{6}\} = [L/2]^2 \setminus \{(0, 3), (1, 2), (2, 1), (3, 0), (4, 5), (5, 4)\}.$$

For the active matrices H_X and H_Z with $J = 3$,

$$H_X H_Z^\top = (\Psi_{(k-i) \bmod 6})_{0 \leq i, k \leq 2} = \begin{pmatrix} \Psi_0 & \Psi_1 & \Psi_2 \\ \Psi_5 & \Psi_0 & \Psi_1 \\ \Psi_4 & \Psi_5 & \Psi_0 \end{pmatrix}.$$

Thus active orthogonality is equivalent to

$$\Psi_r = 0 \quad (r \in \{0, 1, 2, 4, 5\} = \Delta),$$

so the $r = 3$ interaction can be kept free. The mother-matrix product $\hat{H}_X(\hat{H}_Z)^\top$ is

$$\hat{H}_X(\hat{H}_Z)^\top = (\Psi_{(k-i) \bmod 6})_{0 \leq i, k \leq 5} = \left(\begin{array}{ccc|ccc} \Psi_0 & \Psi_1 & \Psi_2 & \Psi_3 & \Psi_4 & \Psi_5 \\ \Psi_5 & \Psi_0 & \Psi_1 & \Psi_2 & \Psi_3 & \Psi_4 \\ \Psi_4 & \Psi_5 & \Psi_0 & \Psi_1 & \Psi_2 & \Psi_3 \\ \hline \Psi_3 & \Psi_4 & \Psi_5 & \Psi_0 & \Psi_1 & \Psi_2 \\ \Psi_2 & \Psi_3 & \Psi_4 & \Psi_5 & \Psi_0 & \Psi_1 \\ \Psi_1 & \Psi_2 & \Psi_3 & \Psi_4 & \Psi_5 & \Psi_0 \end{array} \right).$$

Table 1: Constructed APM parameters ($P = 768, J = 3, L = 12$, girth=8)

i	$f_i(x)$	$g_i(x)$
0	$763x + 435$	$289x + 496$
1	$679x + 69$	$257x + 640$
2	$397x + 330$	$625x + 200$
3	$61x + 18$	$41x + 524$
4	$697x + 612$	$193x + 672$
5	$373x + 246$	$449x + 672$

For the $J = 3, L = 12$ Tanner graph, the block positions

$$[(0, 0), (0, 6), (1, 6), (1, 1), (2, 1), (2, 7), (1, 7), (1, 0)]$$

form an 8-cycle when traversed in order. The corresponding cycle word, in the form of Eq. (1), is

$$W = F_0 G_0^{-1} G_5 F_5^{-1} F_5 G_5^{-1} G_0 F_0^{-1}.$$

6.2 Design goal and commutation table

With $L/2 = 6$ and $J = 3$, we have $\Delta = \{0, 1, 2, 4, 5\}$ (so $3 \notin \Delta$). The design goal is

$$\Psi_r = 0 \quad (r \in \Delta), \quad \Psi_3 \neq 0.$$

This guarantees active orthogonality while breaking mother orthogonality, thereby creating room to prevent the latent part from becoming orthogonal to the active part.

As a schematic commutation table, suppose all pairs (F_i, G_j) commute except $(i, j) = (0, 3), (1, 2)$. The table below shades commuting pairs in Γ with 1:

	G_0	G_1	G_2	G_3	G_4	G_5
F_0	1	1	1	0	1	1
F_1	1	1	0	1	1	1
F_2	1	1	1	1	1	1
F_3	1	1	1	1	1	1
F_4	1	1	1	1	1	1
F_5	1	1	1	1	1	1

Then

$$\Psi_r = 0 \quad (r \neq 3), \quad \Psi_3 = F_0 G_3 + G_3 F_0 + F_1 G_2 + G_2 F_1.$$

A reader might think it is sufficient to keep only Ψ_3 nonzero while setting $\Psi_4 = 0$. We initially considered this and designed the code so that only F_0, G_3 were non-commuting, yielding $\Psi_3 \neq 0$ and $\Psi_4 = 0$. However, this produced many elementary trapping sets (ETS) formed by connecting k length-8 cycles, which are the most harmful [6]. Representative ETSs are shown in Fig. 1. When we instead designed the code so that $\Psi_3 \neq 0$ and $\Psi_4 \neq 0$, making both F_0, G_3 and F_1, G_2 non-commuting, we substantially reduced connected ETSs for $k \leq 10$.

6.3 Affine permutation construction and choice of P

The affine permutations f_i, g_i constructed by the algorithm are listed in Table 1. If P is a prime power, there is no set of permutations $\sigma_0, \sigma_1, \tau_0, \tau_1$ on $[P]$ that simultaneously satisfy: σ_0 commutes

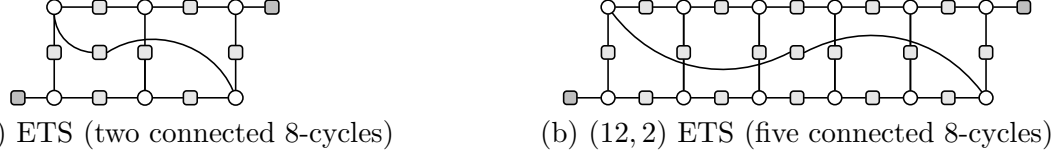


Figure 1: ETSs formed by connecting $k = 2, 5$ length-8 cycles. Filled check nodes have degree 1 (unsatisfied). Counts for $P = 768, J = 3, L = 12$: (6, 2) ETS ($X=48, Z=16$) and (12, 2) ETS ($X=23, Z=0$).

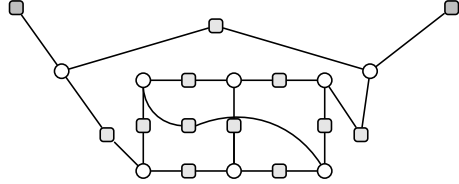


Figure 2: Tanner graph of an ETS with (8,2). The internal subgraph matches the (6,2) ETS in Fig. 1(a), and the length-4 path connects its former degree-1 checks (C0:599 and C0:542). Count for $P = 768, J = 3, L = 12$: (8, 2) ETS ($X=48, Z=0$).

with τ_0 but not with τ_1 , and σ_1 does not commute with τ_0 but commutes with τ_1 . Using the standard semidirect-product representation of $\mathrm{AGL}_1(\mathbb{Z}/p^k\mathbb{Z})$, $(a, b) : x \mapsto ax + b$, and the quadratic commutation condition, one can show this by analyzing the resulting zero-product conditions with p -adic valuation, which contradict non-commutativity. Therefore we choose $P = 768 = 3 \times 2^8$.

6.4 ETS library construction

In our initial experiments, ETSs of the form shown in Fig. 1 were the dominant cause of BP stalls. Since the constructed code has girth 8, we first enumerate 8-cycles and then build an ETS library by connecting 8-cycles to generate ETSs isomorphic to these patterns. The library is not a collection of only the ETSs encountered in decoding; instead, we enumerate all ETSs isomorphic to the dominant patterns and add them exhaustively.

Figure 1(a) is a (6, 2) ETS obtained by connecting two length-8 cycles, and Fig. 1(b) is a (12, 2) ETS obtained by connecting five length-8 cycles. Figure 2 shows a (8, 2) ETS formed by attaching a length-4 check-variable path between the two odd checks of a (6, 2) ETS. For the constructed code with $P = 768, J = 3, L = 12$, the enumerator found (6, 2) ETSs: $X = 48, Z = 16$ (total 64); (12, 2) ETSs: $X = 23, Z = 0$ (total 23); and (8, 2) ETSs of the path4 type: $X = 48, Z = 0$ (total 48).

The parameters f_i, g_i constructed by the algorithm are listed in Table 1 (indices start at 0). Each f_i, g_i is an affine permutation $x \mapsto ax + b$ on \mathbb{Z}_P with $\gcd(a, P) = 1$. The resulting Tanner graph has girth 8 (no 4- or 6-cycles). We also verified that small (a, 2) ETSs obtained by connecting length-8 cycles do not appear up to a prescribed search limit $a \leq A$ (details omitted).

6.5 Minimum-distance evaluation

Let $\mathbf{u}, \mathbf{v} \in \mathbb{F}_2^{3P}$ be coefficient vectors satisfying $\mathrm{diag}(\Psi_3^\top, \Psi_3^\top, \Psi_3^\top)\mathbf{u} = 0$ and $\mathrm{diag}(\Psi_3, \Psi_3, \Psi_3)\mathbf{v} = 0$. Define $\mathbf{x} := \mathbf{u}^\top \tilde{H}_X$ and $\mathbf{z} := \mathbf{v}^\top \tilde{H}_Z$ using the latent matrices \tilde{H}_X and \tilde{H}_Z . Here H_X and H_Z are the active matrices, so $\mathbf{u} \in \mathrm{Ker}(H_Z(\tilde{H}_X)^\top)$ and $\mathbf{v} \in \mathrm{Ker}(H_X(\tilde{H}_Z)^\top)$. With $L/2 = 6, J = 3$ and $\Psi_r = 0$ ($r \neq 3$),

$$H_Z(\tilde{H}_X)^\top = \mathrm{diag}(\Psi_3^\top, \Psi_3^\top, \Psi_3^\top), \quad H_X(\tilde{H}_Z)^\top = \mathrm{diag}(\Psi_3, \Psi_3, \Psi_3).$$

Commutativity makes the terms for $u = 2, 3, 4, 5$ vanish, so

$$\Psi_3 = F_0 G_3 + G_3 F_0 + F_1 G_2 + G_2 F_1,$$

and hence

$$\Psi_3^T = F_0^T G_3^T + G_3^T F_0^T + F_1^T G_2^T + G_2^T F_1^T.$$

Thus Ψ_3 is a sum of four permutation matrices with disjoint supports, so both row and column weights are 4. Therefore any codeword \mathbf{u} of $H_Z(\tilde{H}_X)^T$ decomposes as $\mathbf{u} = (\mathbf{u}_3, \mathbf{u}_4, \mathbf{u}_5)$ where each \mathbf{u}_i is a codeword of $\text{Ker}(\Psi_3^T)$. From the structure of $\text{Ker}(\Psi_3^T)$ and $\text{Ker}(\Psi_3)$, the support splits and weights are multiples of 4. The minimum distance of $\text{Ker}(\Psi_3^T)$ is 4. We confirmed the existence of a weight-48 \mathbf{x} constructed from a weight-4 codeword of Ψ_3^T . Therefore $d_X^{(\text{lat})}, d_Z^{(\text{lat})} \leq 48$, and consequently $d_{\min} \leq 48$. We do not prove a matching lower bound. Randomized searches did not find smaller logical errors, and large-scale decoding experiments did not exhibit logical failures, so we conjecture that this upper bound is tight.

6.6 FER performance

Figure 3 reports the FER of the constructed code under BP with post-processing. For reference, we also include the hashing bound for the depolarizing channel in the plot. At $p = 4\%$, the FER reaches 10^{-8} . For each point we collected at least 50 error events; 95% confidence intervals are plotted but may be visually indistinguishable because they are narrow. For FER above 10^{-7} , all failures left hundreds of remaining errors, and we did not observe cases where the decoder returned low-weight logical errors (including higher-weight ones), which is common in small-distance codes. Around 10^{-8} , an error-floor tendency begins to appear, and the dominant failures are stalls trapped by trapping sets of size on the order of tens.

References

- [1] R. G. Gallager. *Low-Density Parity-Check Codes*. MIT Press, Cambridge, MA, 1963.
- [2] S. Kudekar, T. J. Richardson, and R. L. Urbanke. Spatially coupled ensembles universally achieve capacity under belief propagation. *IEEE Transactions on Information Theory*, 59(12):7761–7813, 2013.
- [3] T. J. Richardson and R. L. Urbanke. The capacity of low-density parity-check codes under message-passing decoding. *IEEE Transactions on Information Theory*, 47(2):599–618, 2001.
- [4] T. J. Richardson, M. A. Shokrollahi, and R. L. Urbanke. Design of capacity-approaching irregular low-density parity-check codes. *IEEE Transactions on Information Theory*, 47(2):619–637, 2001.
- [5] T. J. Richardson and R. L. Urbanke. *Modern Coding Theory*. Cambridge University Press, Cambridge, UK, 2008.
- [6] T. J. Richardson. Error floors of LDPC codes. In *Proc. 41st Annual Allerton Conference on Communication, Control, and Computing*, 2003.
- [7] R. M. Tanner. A recursive approach to low complexity codes. *IEEE Transactions on Information Theory*, 27(5):533–547, 1981.

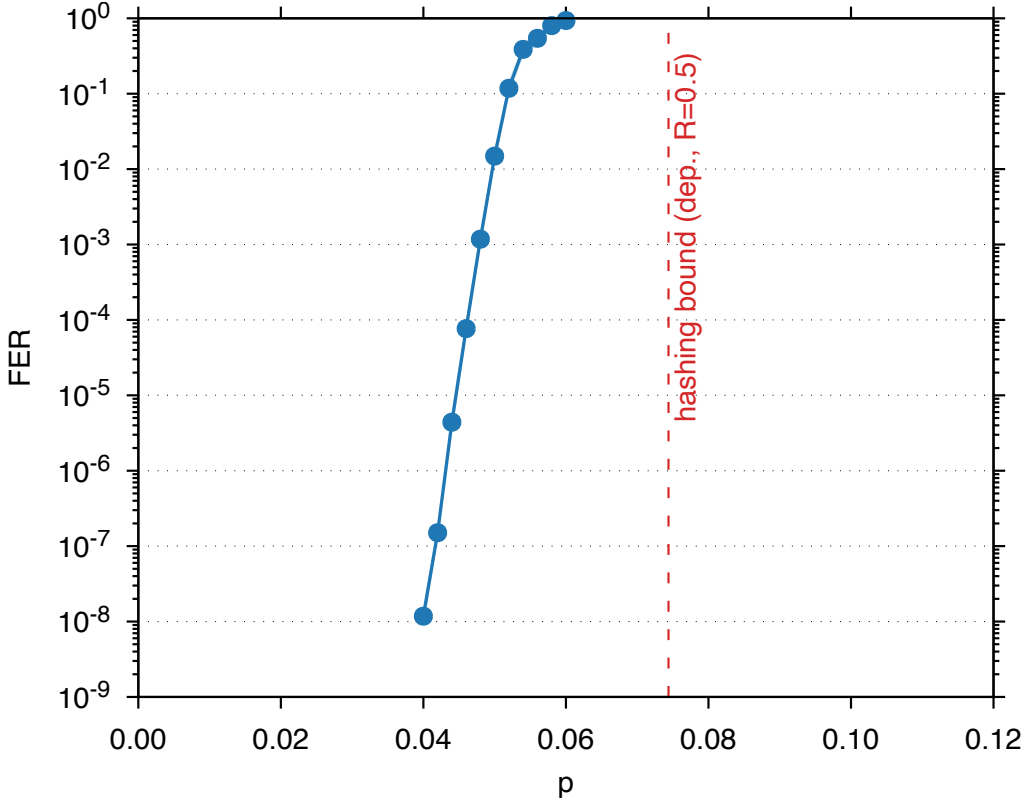


Figure 3: FER curve of the constructed code girth-8, (3,12)-regular $[[9216, 4612, \leq 48]]$, ($P = 768, J = 3, L = 12$) with error bars (95% confidence). Here $n = PL$, the active matrix ranks are $\text{rank}(H_X) = 2302$ and $\text{rank}(H_Z) = 2302$, hence $k = 4612$.

- [8] D. J. C. MacKay, G. Mitchison, and P. L. McFadden. Sparse-graph codes for quantum error correction. *IEEE Transactions on Information Theory*, 50(10):2315–2330, 2004.
- [9] D. Poulin and Y. Chung. On the iterative decoding of sparse quantum codes. *Physical Review A*, 77:012308, 2008.
- [10] J.-P. Tillich and G. Zémor. Quantum LDPC codes with positive rate and minimum distance proportional to the square root of the blocklength. *IEEE Transactions on Information Theory*, 60(2):1193–1202, 2014.
- [11] A. A. Kovalev and L. P. Pryadko. Quantum kronecker sum-product low-density parity-check codes with finite rate. *Physical Review A*, 88:012311, 2013.
- [12] R. Wang and L. P. Pryadko. Distance bounds for generalized bicycle codes. *Symmetry*, 14(7):1348, 2022.
- [13] O. A. Mostad, H.-Y. Lin, E. Rosnes, D.-S. Lee, and C.-Y. Lai. Advancing finite-length quantum error correction using generalized bicycle codes. In *Proc. 13th International Symposium on Topics in Coding (ISTC)*, pages 1–5, Los Angeles, CA, USA, Aug. 2025.
- [14] H.-K. Lin, X. Liu, P. K. Lim, and L. P. Pryadko. Single-shot and two-shot decoding with generalized bicycle codes, 2025. arXiv:2502.19406.

- [15] A. G. Fowler, M. Mariantoni, J. M. Martinis, and A. N. Cleland. Surface codes: Towards practical large-scale quantum computation. *Physical Review A*, 86:032324, 2012.
- [16] M. Hagiwara and H. Imai. Quantum quasi-cyclic LDPC codes. In *Proc. IEEE International Symposium on Information Theory (ISIT)*, pages 806–810, Nice, France, 2007.
- [17] D. G. M. Mitchell, R. Smarandache, and Jr. Costello, D. J. Quasi-cyclic LDPC codes based on pre-lifted protographs. *IEEE Transactions on Information Theory*, 60(10):5856–5874, 2014.
- [18] M.-H. Hsieh, T. A. Brun, and I. Devetak. Entanglement-assisted quantum quasi-cyclic low-density parity-check codes. *Physical Review A*, 79:032340, 2009.
- [19] D. Komoto and K. Kasai. Quantum error correction near the coding theoretical bound. *npj Quantum Information*, 11(1):154, 2025.
- [20] F. Amirzade, D. Panario, and M.-R. Sadeghi. Girth analysis of quantum quasi-cyclic LDPC codes. *Problems of Information Transmission*, 60(2):71–89, 2024.
- [21] K. Kasai. Quantum error correction with girth-16 non-binary LDPC codes via affine permutation construction. In *Proc. 13th International Symposium on Topics in Coding (ISTC)*, pages 1–5, Los Angeles, CA, USA, Aug. 2025.
- [22] D. Ostrev, D. Orsucci, F. Lazaro, and B. Matuz. Classical product code constructions for quantum calderbank–shor–steane codes. *Quantum*, 8:1420, 2024.
- [23] A. R. Calderbank and P. W. Shor. Good quantum error-correcting codes exist. *Physical Review A*, 54(2):1098–1105, 1996.
- [24] A. Steane. Multiple-particle interference and quantum error correction. *Proceedings of the Royal Society of London A*, 452(1954):2551–2577, 1996.
- [25] D. Gottesman. *Stabilizer Codes and Quantum Error Correction*. PhD thesis, California Institute of Technology, 1997. Ph.D. dissertation; available as arXiv:quant-ph/9705052.
- [26] K. Kasai. Quantum error correction exploiting degeneracy to approach the hashing bound, 2025. arXiv:2506.15636.
- [27] J. Thorpe. Low-density parity-check (LDPC) codes constructed from protographs. Technical Report 42-154, IPN, Aug. 2003.
- [28] M. Fossorier. Quasi-cyclic low-density parity-check codes from circulant permutation matrices. *IEEE Transactions on Information Theory*, 50(8):1788–1793, 2004.
- [29] M. Gholami and M. Alinia. High-performance binary and non-binary low-density parity-check codes based on affine permutation matrices. *IET Communications*, 9(17):2114–2123, 2015.
- [30] R. Yoshida and K. Kasai. Linear permutation polynomial codes. In *2019 IEEE International Symposium on Information Theory (ISIT)*, pages 66–70. IEEE, July 2019.
- [31] S. Myung, K. Yang, and D. S. Park. A combining method of structured LDPC codes from affine permutation matrices. In *Proc. IEEE Int. Symp. Information Theory (ISIT)*, pages 674–678, 2006.

- [32] P. Auer, N. Cesa-Bianchi, and P. Fischer. Finite-time analysis of the multiarmed bandit problem. *Machine Learning*, 47(2–3):235–256, 2002.
- [33] J. Zhang and M. P. C. Fossorier. A modified weighted bit-flipping decoding of low-density parity-check codes. *IEEE Communications Letters*, 8(3):165–167, 2004.
- [34] I. Dumer. Soft-decision decoding of linear block codes based on ordered statistics. *IEEE Transactions on Information Theory*, 44(7):2587–2604, 1998.